

# Transformations from cone responses to opponent color spaces

Meiyue Liu<sup>1</sup> | Cheng Gao<sup>1</sup>  | Xiaohui Zhang<sup>1</sup> | Manuel Melgosa<sup>2</sup>  |  
Kaida Xiao<sup>1,3</sup>  | Daniel Vázquez<sup>4</sup> | Changjun Li<sup>1</sup> 

<sup>1</sup>School of Computer and Software Engineering, University of Science and Technology Liaoning, Anshan, China

<sup>2</sup>Department of Optics, University of Granada, Granada, Spain

<sup>3</sup>School of Design, University of Leeds, Leeds, UK

<sup>4</sup>Faculty of Optics and Optometry, Complutense University of Madrid, Madrid, Spain

## Correspondence

Changjun Li, School of Computer and Software Engineering, University of Science and Technology Liaoning, Anshan 114051, China.  
Email: cjliustl@sina.com

## Funding information

Ministry of Science and Innovation of the National Government of Spain, Grant/Award Number: PID2019-107816GB-I00/SRA/10.13039/501100011033; National Natural Science Foundation of China, Grant/Award Numbers: 61575090, 61775169; University of Science and Technology Liaoning; Foundation of Liaoning Province Education Administration

## Abstract

We have described a number of transformations by mapping the cone signal vector  $C$ , formed by  $LMS$ , to opponent space  $O$ , formed by achromatic signal  $O_A$ , red-green signal  $O_{rg}$ , and yellow-blue signal  $O_{yb}$ . Two new transformations,  $\Gamma_{op1}$  and  $\Gamma_{op2}$ , are proposed, based on the CIE 2006 spectral luminous efficiency function,  $V_F(\lambda)$ , and Hurvich's opponent spectral red-green and yellow-blue responses,  $H_{rg}(\lambda)$  and  $H_{yb}(\lambda)$ , without and with constraints, respectively.  $\Gamma_{op1}$  is better than  $\Gamma_{op2}$  in terms of best fit of  $H_{rg}(\lambda)$  and  $H_{yb}(\lambda)$ , and both transformations improved previously proposed ones. Finally, we discuss the *neutral conditions* in cone space using each of the new and some of the extant transformations, as well as choosing scaling factors so that the *neutral conditions* in cone space are satisfied.

## KEYWORDS

cone fundamentals, opponent color space, opponent spectral responses

## 1 | INTRODUCTION

In 2006, the International Commission on Illumination (CIE) recommended 2 and 10° cone fundamental responses.<sup>1-2</sup> Figure 1 shows the CIE 2006 2°  $\bar{l}(\lambda)$  (red),  $\bar{m}(\lambda)$  (green), and  $\bar{s}(\lambda)$  (blue) cone fundamental spectral responses after normalization (ie, when each of the responses has a unity peak). For a given stimulus with spectral radiance  $\varphi(\lambda)$ , cone response signals  $L$ ,  $M$ , and  $S$  are computed from cone fundamental responses using the following equation:

$$\begin{cases} L = \int_a^b \varphi(\lambda) \bar{l}(\lambda) d\lambda \\ M = \int_a^b \varphi(\lambda) \bar{m}(\lambda) d\lambda \\ S = \int_a^b \varphi(\lambda) \bar{s}(\lambda) d\lambda \end{cases} \quad (1)$$

where  $a$  and  $b$  are the lower and upper limits, respectively, of the visible range. Achieving cone response signals  $L$ ,  $M$ , and  $S$  for the spectral radiance  $\varphi(\lambda)$  of a certain stimulus is the first stage for all two-step vision theories. The second stage is to transfer cone signals to an opponent color space, that is, an achromatic signal,

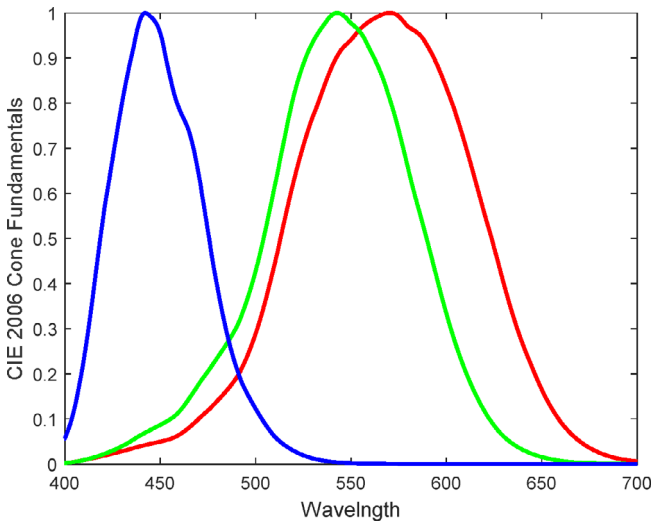


**FIGURE 1** CIE 2006 2° cone fundamentals  $\bar{l}(\lambda)$  (red),  $\bar{m}(\lambda)$  (green), and  $\bar{s}(\lambda)$  (blue), ranging from 400 nm to 700 nm

$O_A$ , and two opponent chromatic signals,  $O_{rg}$  (red-green) and  $O_{yb}$  (yellow-blue). If we let the  $\Gamma$  transform be a three-by-three matrix, the second stage can be described as a matrix and vector multiplication:

$$O = \Gamma C \quad (2)$$

where vector  $C$  is formed by cone response signals, vector  $O$  is formed by signals in opponent color space, and the superscript  $T$  means transpose:

$$C = (L \ M \ S)^T \quad (3)$$

and

$$O = (O_A \ O_{rg} \ O_{yb})^T. \quad (4)$$

Different  $\Gamma$  transforms have been proposed in previous studies. For example, from figure 3 in the paper by Stockman and Brainard,<sup>3</sup> we have

$$\Gamma_{SB} = \begin{pmatrix} 1 & 1 & 0 \\ 1 & -1 & 0 \\ 1 & 1 & -1 \end{pmatrix}. \quad (5)$$

From figure 1.4 in the book by Hunt and Pointer<sup>4</sup> we have

$$\Gamma_{HP} = \begin{pmatrix} 2 & 1 & 1/20 \\ 1 & -1 & 0 \\ 1 & 1 & -2 \end{pmatrix}. \quad (6)$$

From figure 1(8.3.4), p. 647, in the book by Wyszecki and Stiles,<sup>5</sup> we have

$$\Gamma_{WS} = \begin{pmatrix} 1 & 1 & 0 \\ 1 & -1 & 0 \\ 1 & 0 & -1 \end{pmatrix}. \quad (7)$$

In 2020, Wuerger et al<sup>6</sup> proposed

$$\Gamma_W = \begin{pmatrix} 1 & 1 & 0 \\ 1 & -\frac{L_0}{M_0} & 0 \\ 1 & 1 & -\frac{L_0 + M_0}{S_0} \end{pmatrix}, \quad (8)$$

where  $L_0$ ,  $M_0$ , and  $S_0$  are the cone response signals for the neutral background under the given illuminant.

In 2021, from similarities in wavelength peaks in 16 studies of cone responses and 15 studies of opponent chromatic responses, Pridmore<sup>7</sup> proposed the following matrix for obtaining the two color opponent signals,  $O_{rg}$  and  $O_{yb}$ , from vector  $C$  in Equation (3):

$$\Gamma_P = \begin{pmatrix} 1 & -1 & 1 \\ 1 & 0 & -1 \end{pmatrix} \quad (9)$$

Recently, the CIE has set up its Technical Committee (TC) 1-98, "A roadmap towards basing CIE colorimetry on cone fundamentals," for studying the establishment of a new colorimetry based on cone response signals. As we have learned from current CIE colorimetry, developed from CIE color-matching functions, an opponent color space (eg, the CIELAB color space) is a key tool for the theoretical and practical applications of color science.<sup>8</sup> The currently unsolved problem is which transform should be used for transforming cone response signals to opponent color signals. In this article, we want to evaluate the above-mentioned transforms in terms of their fitting both the CIE spectral luminous efficiency function and the opponent chromatic spectral response signals reported by Hurvich.<sup>9</sup> Figure 2 shows Hurvich's opponent signals:  $H_{rg}(\lambda)$  (solid curve) is the red-green spectral response and  $H_{yb}(\lambda)$  (dotted curve) is the yellow-blue spectral response. More specifically, by using these

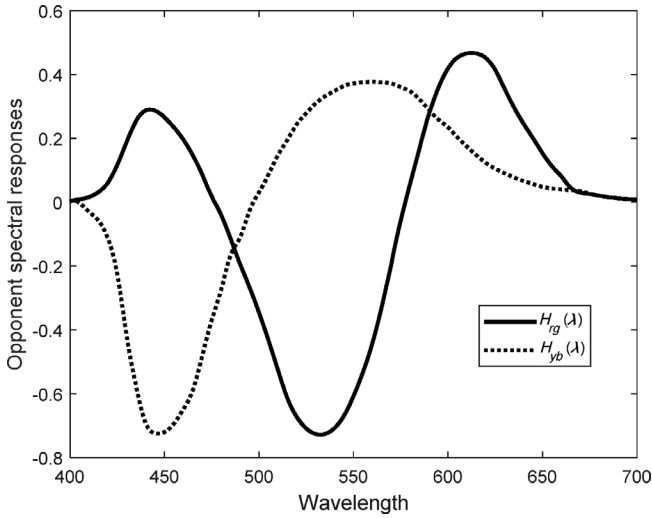


**FIGURE 2** Opponent red-green  $H_{rg}(\lambda)$  and yellow-blue  $H_{yb}(\lambda)$  spectral responses redrawn from Hurvich<sup>9</sup>

valuable experimental data sets as references, in the current paper we will develop two new  $\Gamma$  transforms (see Equation (2)), and discuss the *neutral conditions* in cone space for using each of the transforms defined by Equations (5)–(9) and the new transforms. We will also discuss how to choose scaling factors so that the *neutral conditions* in cone space are satisfied.

## 2 | NEW TRANSFORMS

Firstly, from Equation (2), if we let

$$C = c(\lambda) = (\bar{l}(\lambda) \quad \bar{m}(\lambda) \quad \bar{s}(\lambda))^T, \quad (10)$$

the achromatic and opponent  $O$  signals are also dependent on the wavelength. Hence, we will let

$$O = o(\lambda) = (o_A(\lambda) \quad o_{rg}(\lambda) \quad o_{yb}(\lambda))^T, \quad (11)$$

Since  $O_A$  is the achromatic signal in the opponent color space, we can expect  $o_A(\lambda)$  to be close to the spectral luminous function. Several spectral luminous efficiency functions are available, including the Judd extension,<sup>10</sup> the CIE 1931 color-matching function  $\bar{y}(\lambda)$ , and the  $V_F(\lambda)$ , based on CIE 2006 2° cone fundamentals.<sup>1–2</sup> Since this article focuses on cone fundamentals, we have chosen the  $V_F(\lambda)$  function as our reference.

Let  $o_{A1}(\lambda) = o_A(\lambda)$ , obtained using the transforms defined by Equations (5), (7), or (8), and  $o_{A2}(\lambda) = o_A(\lambda)$ , obtained using the transform defined by Equation (6).

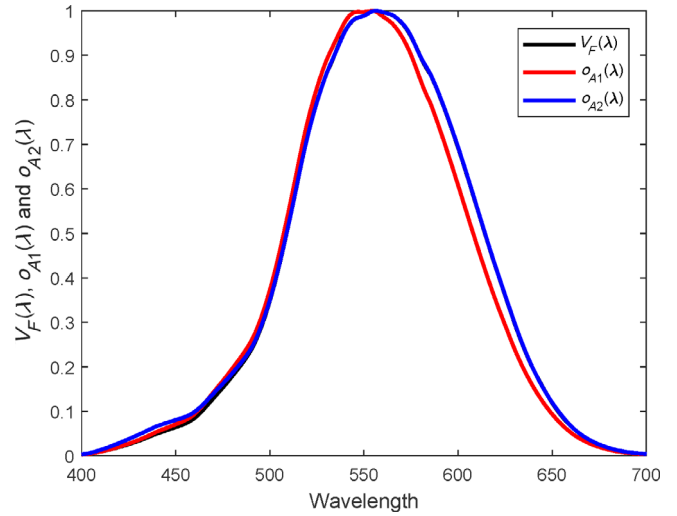


**FIGURE 3** The CIE spectral luminous efficiency function  $V_F(\lambda)$  (black), plus two normalized (unity peak) functions,  $o_{A1}(\lambda)$  (red) and  $o_{A2}(\lambda)$  (blue) (see main text), ranging from 400 nm to 700 nm

Figure 3 shows  $V_F(\lambda)$  (black), as well as the normalized (unity peak)  $o_{A1}(\lambda)$  (red) and  $o_{A2}(\lambda)$  (blue) functions. As we can see, the normalized  $o_{A1}(\lambda)$  (red) and  $o_{A2}(\lambda)$  (blue) functions are quite close to  $V_F(\lambda)$  (black). In particular,  $V_F(\lambda)$  (black) and  $o_{A2}(\lambda)$  (blue) nearly overlap for wavelengths greater than 475 nm. In fact, from CIE,<sup>1–2</sup> we have:

$$V_F(\lambda) = 0.68990272\bar{l}(\lambda) + 0.34832189\bar{m}(\lambda). \quad (12)$$

Hence, if the desired  $\Gamma$  transform (Equation (2)) has the general form of

$$\Gamma = \begin{pmatrix} t_{11} & t_{12} & t_{13} \\ t_{21} & t_{22} & t_{23} \\ t_{31} & t_{32} & t_{33} \end{pmatrix}, \quad (13)$$

then the best choice for the first row of  $\Gamma$  is:

$$(t_{11} \quad t_{12} \quad t_{13}) = (0.68990272 \quad 0.34832189 \quad 0). \quad (14)$$

Next, we will consider the two opponent red-green,  $O_{rg}$ , and yellow-blue,  $O_{yb}$ , signals. When we consider that  $C = c(\lambda)$ , defined by Equation (10), we can expect that  $o_{rg}(\lambda)$  and  $o_{yb}(\lambda)$  (see Equation (11)) will be close to the red-green  $H_{rg}(\lambda)$  and yellow-blue  $H_{yb}(\lambda)$  spectral responses (see Figure 2), respectively.

Let us consider the red-green channel first. From Equations (5)–(8) and (13), the first case (denominated RG-Case1) for the transform is

$$(t_{21} \ t_{22} \ t_{23}) = (1 \ -x \ 0). \quad (15)$$

When  $x = 1$ , the situation is that of Equations (5)-(7), and when  $x = \frac{L_0}{M_0}$ , the situation is that of Equation (8). We computed the best  $x$  so that  $o_{rg}(\lambda)$  is closest to  $H_{rg}(\lambda)$ , and it was found that  $x = 1.50273093$ .

From Equation (9) (denominated RG-Case2) we have

$$(t_{21} \ t_{22} \ t_{23}) = (1 \ -1 \ 1). \quad (16)$$

In addition, we computed the best  $(t_{21} \ t_{22} \ t_{23})$  so that  $o_{rg}(\lambda)$  is closest to  $H_{rg}(\lambda)$  (denominated RG-Case3), resulting in a least squares problem<sup>11</sup> with the following solution:

$$(t_{21} \ t_{22} \ t_{23}) = (1.19285019 \ -1.74043682 \ 0.35227109). \quad (17)$$

The fourth case (denominated RG-Case4) was to find the best  $(t_{21} \ t_{22} \ t_{23})$  so that  $o_{rg}(\lambda)$  is closest to  $H_{rg}(\lambda)$  with constraint by the following Equation (18):

$$t_{21} + t_{22} + t_{23} = 0, \quad (18)$$

resulting in a constrained least squares problem<sup>11</sup> with the solution:

$$(t_{21} \ t_{22} \ t_{23}) = (1.20150523 \ -1.67794634 \ 0.47644111). \quad (19)$$

Note that the above constraint (Equation (18)) and the constraint considered later (Equation (25)) are for the  $\Gamma$  transform (see Equation (2)), mapping neutral in LMS cone space to neutral in opponent color space, with the neutral signals  $L_0$ ,  $M_0$ , and  $S_0$  satisfying  $S_0 = L_0 = M_0$ . This is widely used in the color and vision community<sup>4-5</sup> and will be further considered in the next section.

Figure 4 shows Hurvich's opponent red-green function  $H_{rg}(\lambda)$  (black), and the red-green spectral responses achieved from RG-Case1 (red), RG-Case2 (blue), RG-Case3 (magenta), and RG-Case4 (yellow). It can be clearly seen that their order of closeness to the black curve is: magenta, yellow, red, and blue. Hence, RG-Case3 is the best, followed by RG-Case4, RG-Case1, and RG-Case2.

We can measure the closeness between  $H_{rg}(\lambda)$  and the red-green spectral responses achieved by each of our four above cases by using different tools, such as the root mean square error (RMSE)<sup>12</sup> or the goodness of fit coefficient (GFC) used in previous literature.<sup>13</sup> Let  $q$  be a vector with  $n$  elements, and  $p$  an approximation to  $q$ , also

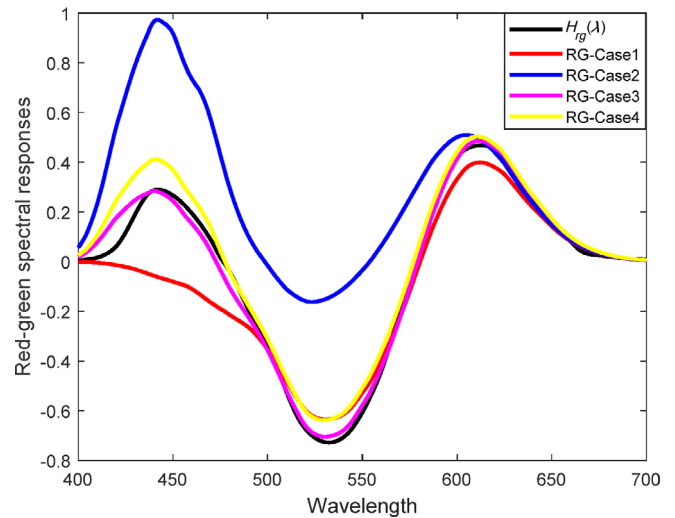


**FIGURE 4** Hurvich's opponent red-green  $H_{rg}(\lambda)$  function (black), together with the red-green spectral responses from RG-Case1, RG-Case2, RG-Case3, and RG-Case4, respectively (see main text)

with  $n$  elements. RMSE and GFC between  $q$  and  $p$  are defined by:

$$\text{RMSE} = \sqrt{\frac{1}{n} \sum_{i=1}^n (q_i - p_i)^2} \quad (20)$$

and

$$\begin{aligned} \text{GFC} &= q^T p / (\|q\|_2 \|p\|_2) \quad \text{with} \quad \|q\|_2 = \sqrt{\sum_{i=1}^n (q_i)^2}, \quad \|p\|_2 \\ &= \sqrt{\sum_{i=1}^n (p_i)^2}. \end{aligned} \quad (21)$$

Thus, if  $q = p$ , RMSE = 0. The closer  $p$  and  $q$  are, the smaller RMSE is. For GFC, it is always equal or smaller than 1, and the closer to 1 the better the agreement between  $p$  and  $q$ . Table 1 lists the RMSE (column 2) and GFC (column 3) values between Hurvich's opponent red-green function  $H_{rg}(\lambda)$  and the spectral responses achieved for each of our four cases. It can be seen from both measurements that the four cases, ordered from best to worst, are RG-Case3, RG-Case4, RG-Case1, and RG-Case2, which is in agreement with the results shown in Figure 4.

Note that from Equation (15) with  $x = 1.50273093$  for RG-Case1, we cannot expect the transforms  $\Gamma_{SB}$ ,  $\Gamma_{HP}$ ,  $\Gamma_{WS}$ , and  $\Gamma_W$  (Equations (5)-(8)) to perform better than

**TABLE 1** RMSE<sup>12</sup> and GFC<sup>13</sup> values between Hurvich's opponent red-green (RG) and yellow-blue (YB) functions and the four corresponding models (Case1-Case4) considered in the current article (see main text)

	RG		YB	
	RMSE	GFC	RMSE	GFC
Case1	0.139	0.920	0.800	0.754
Case2	0.391	0.475	0.369	0.907
Case3	<b>0.047</b>	<b>0.991</b>	<b>0.075</b>	<b>0.971</b>
Case4	0.085	0.970	0.127	0.914

Note: The numbers in bold indicate the best cases in the corresponding row in the first column under the measures shown in the row for RMSE and GFC in corresponding column.

RG-Case3 and RG-Case4, in terms of fitting Hurvich's opponent red-green function,  $H_{rg}(\lambda)$ . Similarly, RG-Case2, corresponding to the transform  $\Gamma_P$  (Equations (9) and (16)), is not expected to perform better than RG-Case3 and RG-Case4 in terms of fitting Hurvich's opponent red-green function  $H_{rg}(\lambda)$ .

We next considered the yellow-blue channel, and distinguished four cases as well. The first, denominated YB-Case1, is the following:

$$(t_{31} \ t_{32} \ t_{33}) = (1 \ 1 \ -y). \quad (22)$$

When  $y = 1$ ,  $y = 2$ , and  $y = -\frac{L_0 + M_0}{S_0}$ , we are presented with the situations indicated in previous Equations (5), (6), and (8), respectively. The best  $y$  value for  $o_{yb}(\lambda)$ , in order of closeness to  $H_{yb}(\lambda)$ , is  $y = 0.92299502$ .

The second case, denominated YB-Case2, is the following:

$$(t_{31} \ t_{32} \ t_{33}) = (1 \ 0 \ -1). \quad (23)$$

This case was given by Equation (7) and by Equation (9) in the recent paper<sup>7</sup> by Pridmore.

The third case, denominated YB-Case3, is to find the best  $(t_{31} \ t_{32} \ t_{33})$  so that  $o_{yb}(\lambda)$  is closest to  $H_{yb}(\lambda)$ . Again, we must solve a least squares problem<sup>11</sup> and it was found that

$$(t_{31} \ t_{32} \ t_{33}) = (0.24289310 \ 0.13401208 \ -0.69913752). \quad (24)$$

Finally, in the fourth case, denominated YB-Case4, we computed the best  $(t_{31} \ t_{32} \ t_{33})$  so that  $o_{yb}(\lambda)$  is closest to  $H_{yb}(\lambda)$ , with the constraint defined by the following Equation (25):

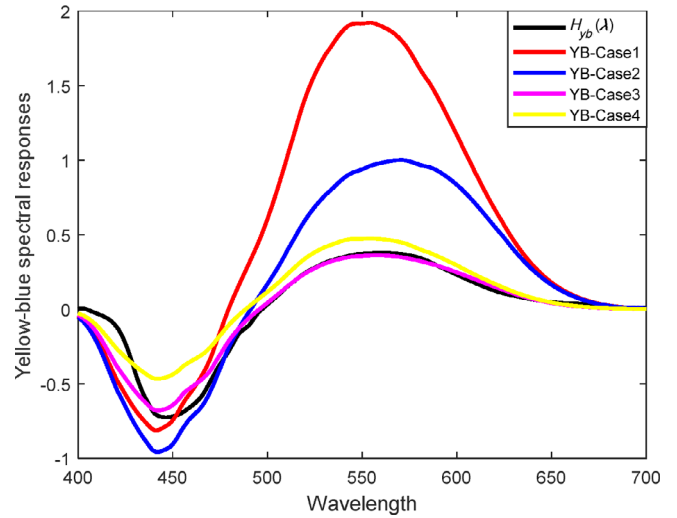


**FIGURE 5** Hurvich's opponent yellow-blue  $H_{yb}(\lambda)$  function (black), together with the yellow-blue spectral responses from YB-Case1, YB-Case2, YB-Case3, and YB-Case4, respectively (see main text)

$$t_{31} + t_{32} + t_{33} = 0. \quad (25)$$

In this last case it was found that

$$(t_{31} \ t_{32} \ t_{33}) = (0.25717223 \ 0.23710911 \ -0.49428134). \quad (26)$$

As noted above, constraints in Equations (18) and (25) allow the  $\Gamma$  transform (see Equation (2)) to map the neutral in  $L$ ,  $M$  and  $S$  space to the neutral in opponent space when the neutral stimulus signals  $L_0$ ,  $M_0$ , and  $S_0$  satisfy  $S_0 = L_0 = M_0$ .

Figure 5 shows Hurvich's opponent yellow-blue spectral function,  $H_{yb}(\lambda)$  (black), together with the yellow-blue spectral responses found from YB-Case1 (red), YB-Case2 (blue), YB-Case3 (magenta), and YB-Case4 (yellow). It can be observed that their order of closeness to the black curve is: magenta, yellow, blue, and red. Hence, YB-Case3 is the best, followed by YB-Case4, YB-Case2, and YG-Case1.

Table 1 lists the RMSE (column 4) and GFC (column 5) values between Hurvich's opponent yellow-blue spectral function  $H_{yb}(\lambda)$  and the yellow-blue spectral responses achieved for each of our four cases. It can be seen from both measurements that the best cases are YB-Case3, YB-Case4, YB-Case2, and YB-Case1, in this order, which is consistent with the results observed in Figure 5.

Note that from Equation (22) with  $y = 0.92299502$  for YB-Case1 we cannot expect transforms  $\Gamma_{SB}$ ,  $\Gamma_{HP}$ , and  $\Gamma_W$

(Equations (5), (6), (8)) to perform better than for YB-Case3 and YB-Case4 in terms of fitting Hurvich's opponent yellow-blue function  $H_{yb}(\lambda)$ . In addition, for YB-Case2, corresponding to transforms  $\Gamma_{WS}$  and  $\Gamma_P$ , we cannot expect these to have a better performance than for YB-Case3 and YB-Case4 in terms of their fitting Hurvich's opponent yellow-blue function  $H_{yb}(\lambda)$ .

From all the above discussions, we can conclude that the best transform is based on Equation (14) for the achromatic signal, Equation (17) for the red-green signal, and Equation (24) for the yellow-blue signal. We have named this transform  $\Gamma_{op1}$ , given by:

$$\Gamma_{op1} = \begin{pmatrix} 0.68990272/k_L & 0.34832189/k_M & 0 \\ 1.19285019 & -1.74043682 & 0.35227109 \\ 0.24289310 & 0.13401208 & -0.69913752 \end{pmatrix}. \quad (27)$$

Similarly, we can point out that the second best transform, denominated  $\Gamma_{op2}$ , is the one achieved from Equations (14), (19), and (26):

$$\Gamma_{op2} = \begin{pmatrix} 0.68990272/k_L & 0.34832189/k_M & 0 \\ 1.20150523 & -1.67794634 & 0.47644111 \\ 0.25717223 & 0.23710911 & -0.49428134 \end{pmatrix}. \quad (28)$$

Here,  $k_L$ ,  $k_M$  (and  $k_S$ ) are scaling factors used to compute the cone response signals (see Equation (1)) that will be considered in the next section (see Equation (32)). Up to now, we have assumed that  $k_L = 1$  and  $k_M = 1$  have the best fit for the spectral luminous efficiency function  $V_F(\lambda)$ .

Note that the above analyses and proposed new transforms used the Hurvich's opponent response functions<sup>9</sup> as reference. Although different sets of opponent response functions are available in the literature (see Table 1 in reference 7), we used Hurvich's opponent response functions because they have been widely used in previous literature, including the recent article by Pridmore (figure 2 in reference 7).

### 3 | DISCUSSIONS AND CONCLUSIONS

In color science, an  $\Gamma$  transform is useful if  $O = \Gamma C$  maps the neutral color vector  $C_0 = (L_0 \ M_0 \ S_0)^T$  to opponent space  $O = (O_A \ O_{rg} \ O_{yb})^T$  with  $O_{rg} = 0$  and  $O_{yb} = 0$ , which is referred to as a *neutral-to-neutral condition* for

the  $\Gamma$  transform considered. It can be verified that the  $\Gamma_W$  transform given by Wuerger et al<sup>6</sup> (see Equation (8)) always satisfies this condition. However, for the other transforms described here we can deduce the *neutral condition* in cone space for the neutral color vector  $C_0 = (L_0 \ M_0 \ S_0)^T$  using this *neutral-to-neutral condition*.

For example, when using the transform  $\Gamma_{SB}$  defined by Equation (5), to obtain  $O_{rg} = 0$  and  $O_{yb} = 0$  we must have the *neutral condition* in cone space:

$$L_0 = M_0 \text{ and } S_0 = 2L_0 = 2M_0. \quad (29)$$

Note that when using the transforms  $\Gamma_{HP}$ ,  $\Gamma_{WS}$ , and  $\Gamma_{op2}$ , defined by Equations (6), (7), (28), respectively, the sum of the coefficients in the second and third rows of the matrices is zero, and hence, the *neutral-to-neutral condition* is fulfilled when the neutral color vector  $C_0$  satisfies

$$S_0 = L_0 = M_0. \quad (30)$$

For the transform  $\Gamma_P$ , defined by Equation (9), the *neutral-to-neutral condition* is fulfilled if the neutral color vector  $C_0$  satisfies

$$S_0 = L_0, M_0 = 2L_0 = 2S_0. \quad (31)$$

To allow the neutral color stimulus to satisfy any of the neutral conditions defined by Equations (29)-(31), we must introduce the scaling factors  $k_L$ ,  $k_M$ , and  $k_S$  into Equation (1) to compute the cone response signals  $LMS$ , so that

$$\begin{cases} L = k_L \int_a^b \varphi(\lambda) \bar{l}(\lambda) d\lambda \\ M = k_M \int_a^b \varphi(\lambda) \bar{m}(\lambda) d\lambda \\ S = k_S \int_a^b \varphi(\lambda) \bar{s}(\lambda) d\lambda \end{cases} \quad (32)$$

Let  $\varphi_0(\lambda)$  be the spectral radiance for a given neutral stimulus. Then, in order to satisfy the *neutral condition* Equation (29) in cone space, the scaling factors  $k_L$ ,  $k_M$ , and  $k_S$  in Equation (32) are determined by the following Equation (33) for a given constant  $c$  (eg,  $c = 1$  or  $100$ ):

$$\begin{aligned} k_L \int_a^b \varphi_0(\lambda) \bar{l}(\lambda) d\lambda &= k_M \int_a^b \varphi_0(\lambda) \bar{m}(\lambda) d\lambda = c \\ &= 0.5k_S \int_a^b \varphi_0(\lambda) \bar{s}(\lambda) d\lambda \end{aligned} \quad (33)$$

In order to satisfy the *neutral condition* Equation (30) in cone space, the scaling factors  $k_L$ ,  $k_M$ , and  $k_S$  in Equation (32) are determined by the following Equation (34) for a given constant  $d$  (eg,  $d = 1$  or  $100$ ):

$$k_L \int_a^b \varphi_0(\lambda) \bar{l}(\lambda) d\lambda = k_M \int_a^b \varphi_0(\lambda) \bar{m}(\lambda) d\lambda = k_S \int_a^b \varphi_0(\lambda) \bar{s}(\lambda) d\lambda = d \quad (34)$$

However, in order to satisfy the *neutral condition* Equation (31) in cone space, the scaling factors  $k_L$ ,  $k_M$ , and  $k_S$  in Equation (32) are determined by the following Equation (35) for a given constant  $f$  (eg,  $f = 1$  or  $100$ ):

$$k_L \int_a^b \varphi_0(\lambda) \bar{l}(\lambda) d\lambda = k_S \int_a^b \varphi_0(\lambda) \bar{s}(\lambda) d\lambda = f = 0.5 k_M \int_a^b \varphi_0(\lambda) \bar{m}(\lambda) d\lambda \quad (35)$$

Determining the scaling factors can also be done by using the newly derived transform  $\Gamma_{op1}$ . Let the second and third rows of the transform  $\Gamma_{op1}$  form a matrix  $A$ . Then we find the singular value decomposition<sup>11</sup> for  $A$ :  $A = UDV^T$ . Here, the superscript  $T$  is the transpose of a matrix, while  $U$  and  $V$  are 2-by-2 and 3-by-3 orthogonal matrices, respectively. The two-by-three matrix  $D$  has a special form, given by:

$$D = \begin{pmatrix} \sigma_1 & 0 & 0 \\ 0 & \sigma_2 & 0 \end{pmatrix} \quad (36)$$

where  $\sigma_1$  and  $\sigma_2$  are the singular (nonnegative) values of the matrix  $A$ .

Let  $v$  be the third column of the orthogonal matrix  $V$ . It can then be verified that  $Av = (0 \ 0)^T$ . In fact,

$$v = (0.73201193 \ 0.57550407 \ 0.36462803)^T. \quad (37)$$

Hence, the *neutral-to-neutral condition* using the transform  $\Gamma_{op1}$  is satisfied if the neutral color vector  $C_0$  satisfies

$$C_0 = (L_0 \ M_0 \ S_0)^T = v. \quad (38)$$

In the preceding, we have discussed the *neutral-to-neutral conditions* for several different transforms. A transform is useful if the associated *neutral-to-neutral condition* is satisfied. We have also discussed the *neutral condition* in cone space for each of the transforms considered, and how to choose the scaling factors  $k_L$ ,  $k_M$ , and  $k_S$  to satisfy these *neutral conditions*. However, different applications may require different *neutral conditions* in

cone space, which may limit the choice of transforms. In color science, a widely accepted *neutral condition* is that the three channel response values  $L_0$ ,  $M_0$ ,  $S_0$  are equal, resulting in the *neutral condition* in Equation (30), which ensures that transforms  $\Gamma_{HP}$  (see Equation (6)),  $\Gamma_{WS}$  (see Equation (7)), and  $\Gamma_{op2}$  (see Equation (28)) satisfy the *neutral-to-neutral condition*. Among these three transforms,  $\Gamma_{op2}$  is the best in terms of fitting the spectral luminous efficiency function  $V_F(\lambda)$  and Hurvich's opponent red-green and yellow-blue responses,  $H_{rg}(\lambda)$  and  $H_{yb}(\lambda)$ .

When the three cone response values  $L_0$ ,  $M_0$ ,  $S_0$  do not satisfy any of the *neutral conditions* given by Equations (29)-(31) and (38) in cone response space, for a particular application the transform  $\Gamma_W$  (see Equation (8)) can be used, as this transform does satisfy the *neutral-to-neutral condition* for any *neutral stimulus* in cone space. However, in this case, a better transform can be developed in terms of fitting of the spectral luminous efficiency function  $V_F(\lambda)$  and Hurvich's opponent red-green and yellow-blue responses,  $H_{rg}(\lambda)$  and  $H_{yb}(\lambda)$ . In fact, if we let the transform be  $\Gamma_{op3}$ , having 9 parameters (see Equation (13)), the first row of  $\Gamma_{op3}$  is the same as the first row of  $\Gamma_{op1}$  (or  $\Gamma_{op2}$ ), and the second and third rows of  $\Gamma_{op3}$  should satisfy:

$$\begin{pmatrix} H_{rg}(\lambda) \\ H_{yb}(\lambda) \end{pmatrix} = \begin{pmatrix} t_{21} & t_{22} & t_{23} \\ t_{31} & t_{32} & t_{33} \end{pmatrix} c(\lambda), \quad (39)$$

where  $c(\lambda)$  is defined by Equation (10). Furthermore, the second and third rows of  $\Gamma_{op3}$  should satisfy the following constraint:

$$\begin{pmatrix} 0 \\ 0 \end{pmatrix} = \begin{pmatrix} t_{21} & t_{22} & t_{23} \\ t_{31} & t_{32} & t_{33} \end{pmatrix} C_0, \quad (40)$$

where  $C_0 = (L_0 \ M_0 \ S_0)^T$ . Note that condition in Equation (39) must be satisfied for each wavelength  $\lambda$ , and hence we need to find a least squares solution for Equation (39). Condition in Equation (40) is the *neutral-to-neutral condition* for the transform  $\Gamma_{op3}$ , and so the final transform can be obtained by solving a constrained least squares problem.<sup>11</sup>

In conclusion, we have examined several transforms (see Equations (5)-(9)) mapping the cone signal vector  $C$  formed by *LMS* to opponent color space  $O$  (see Equations (2)-(4)). We have also derived two new transforms, designated as  $\Gamma_{op1}$  (Equation (27)) and  $\Gamma_{op2}$  (Equation (28)), based on the fit of the CIE spectral luminous efficiency function  $V_F(\lambda)$  and Hurvich's opponent red-green and yellow-blue responses,  $H_{rg}(\lambda)$  and  $H_{yb}(\lambda)$ , without and with constraints (see Equations (18) and

(25)), respectively.  $\Gamma_{op1}$  is better than  $\Gamma_{op2}$  in terms of best fit for  $H_{rg}(\lambda)$  and  $H_{yb}(\lambda)$ . Both  $\Gamma_{op1}$  and  $\Gamma_{op2}$  are better than any of the transforms previously proposed (Equations (5)-(9)), in terms of fit of Hurvich's red-green and yellow-blue opponent spectral responses. Using the transform  $\Gamma_{op1}$ , the *neutral-to-neutral condition* requires that the scaling factors  $k_L$ ,  $k_M$ , and  $k_S$  must be determined so that a *neutral stimulus* in cone space is obtained (Equations (37)-(38)). For the transform  $\Gamma_{op2}$ , the *neutral-to-neutral condition* requires that the scaling factors  $k_L$ ,  $k_M$ , and  $k_S$  be determined so that the *neutral condition* in Equation (30) be satisfied. If the *neutral condition* in cone space is different from that defined by Equations (30) or (38), an  $\Gamma_{op3}$  transform can be obtained by solving the constrained least squares problem defined by Equations (39) and (40).

## ACKNOWLEDGMENTS

This work has been supported by the National Natural Science Foundation of China (grant numbers: 61575090, 61775169), the Ministry of Science and Innovation of the National Government of Spain (Grant number: PID2019-107816GB-I00/SRA/10.13039/501100011033), the Foundation of Liaoning Province Education Administration, and the graduate education reform, scientific and technological innovation, and entrepreneurship project of the University of Science and Technology Liaoning. English assistance from Mr Donald J, Murphy McVeigh is acknowledged.

## DATA AVAILABILITY STATEMENT

The data used to support the findings of this study are available from the corresponding author upon request. The data are not publicly available due to privacy restrictions.

## ORCID

Cheng Gao  <https://orcid.org/0000-0003-2233-2914>

Manuel Melgosa  <https://orcid.org/0000-0002-7226-4190>

Kaida Xiao  <https://orcid.org/0000-0001-7197-7159>

Changjun Li  <https://orcid.org/0000-0002-9942-7690>

## REFERENCES

- [1] CIE. *Fundamental Chromaticity Diagram with Physiological Axes—Part 1*. CIE 170-1:2006. Vienna, Austria: CIE; 2006.
- [2] CIE. *Fundamental Chromaticity Diagram with Physiological Axes—Part 2: Spectral Luminous Efficiency Functions and Chromaticity Diagrams*. CIE 170-2:2015. Vienna, Austria: CIE; 2015.
- [3] Stockman A, Brainard DH. Color Vision Mechanisms. In: Bass M, ed. *OSA Handbook of Optics*. 3rd ed. New York: McGraw-Hill; 2010:11.1-11.104.
- [4] Hunt RWG, Pointer MR. *Measuring Colour*. 4th ed. New York: Wiley; 2011.
- [5] Wyszecki G, Stiles WS. *Color Science: Concepts and Methods, Quantitative Data and Formulae*. 2nd ed. New York: Wiley; 2000.
- [6] Wuerger S, Ashraf M, Kim M, Martinovic J, Pérez-Ortiz M, Mantiuk RK. Spatio-chromatic contrast sensitivity under mesopic and photopic light levels. *J Vis*. 2020;20(4):1-26.
- [7] Pridmore RW. A new transformation of cone responses to opponent color responses. *Atten Percept Psychophys*. 2021;83:1797-1803.
- [8] CIE. *Colorimetry*. CIE 015:2018. 4th ed. Vienna, Austria: CIE; 2018.
- [9] Hurvich LM. *Color Vision*. Sunderland, MA: Sinauer Associates; 1981. Figure on p. 62.
- [10] CIE. *CIE 1988 2° Spectral Luminous Efficiency Function for Photopic Vision*. CIE 086:1990. Vienna, Austria: CIE; 1990.
- [11] Golub GH, Loan CV. *Matrix Computation*. 4th ed. Baltimore, MD: The Johns Hopkins University Press; 2013.
- [12] Carreres-Prieto D, García JT, Cerdán-Cartagena F, Suardiaz-Muro J. Performing calibration of transmittance by single RGB-LED within the visible spectrum. *Sensors*. 2020;20(12):3492.
- [13] Hernández-Andrés J, Romero J, Lee RL. Colorimetric and spectroradiometric characteristics of narrow-field-of-view clear skylight in Granada. *J Opt Soc Am A*. 2001;18(2):412-420.

## AUTHOR BIOGRAPHIES

**Meiyue Liu** is a graduate student in the Department of Computer Science, University of Science and Technology Liaoning, Anshan, China, where she received a BS degree in computer science in 2019. Her current research interests are color and imaging science.

**Cheng Gao** is a research assistant in the Department of Computer Science, University of Science and Technology Liaoning. He received BS (2015), and MS (2018) degrees in software engineering from this university. His current research interests are spectrum optimization of LED, color appearance modeling, and mesopic luminance computation.

**Xiaohui Zhang** is a research assistant in the Department of Software Engineering, University of Science and Technology Liaoning. He received BS (2017), and MS (2020) degrees, respectively, from this university. His current research interests are color and imaging science.

**Manuel Melgosa** is Full Professor in optics at the University of Granada, Spain, and Associate Editor of this journal. Currently he is the Vice-president of International Affairs of the Lighting Committee of Spain, and the Secretary of the Color Vision and Psychophysics Study Group of the International Color Association. He is also the representative of Spain at CIE Divisions 1 and 8, serving as member of CIE TCs

1-98, 8-14, 8-17, 8-18, JTC 10 (D1/D8), and R1-60. His main research interests are color-difference evaluation and applied colorimetry.

**Kaida Xiao** is an associate professor in the Colour and Imaging Science Department in the School of Design, University of Leeds, UK. His research interests are three-dimensional (3D) color image reproduction, 3D color printing, 3D printing facial prostheses, medical image capture and analysis, color appearance modeling, and image quality enhancement.

**Daniel Vázquez** has been Professor in the Optics Department of the Universidad Complutense of Madrid, Spain since 1988. He received a PhD in architecture by Universidad Politécnica of Madrid, Spain. He works in the development of lighting systems applied to several fields such as natural lighting devices, signals, LEDs, and solar energy. His current interests include color perception and lighting systems applied to cultural heritage. Among his works it can be mentioned studies of Portico de la Gloria gate in Santiago de Compostela, Guernica picture in Reina

Sofia Museum of Madrid, and Altamira cave in Cantabria.

**Changjun Li** is Professor in the Department of Computer Science, University of Science and Technology Liaoning, Anshan, China. He received BS (1979), MS (1982), PhD (1989) degrees in computational mathematics from Peking University (China), Chinese Academy of Science, and Loughborough University (UK), respectively. His current research interests are chromatic adaptation transform, color appearance modeling, uniform color spaces, and computational color constancy. Currently he is the Chair of CIE JTC10 on CIECAM16.

**How to cite this article:** Liu M, Gao C, Zhang X, et al. Transformations from cone responses to opponent color spaces. *Color Res Appl.* 2022;47(2): 243-251. doi:10.1002/col.22732